



HAL
open science

Non-volatile SRAM memory cells based on ReRAM technology

Hussein Bazzi, Adnan Harb, Hassen Aziza, Mathieu Moreau

► **To cite this version:**

Hussein Bazzi, Adnan Harb, Hassen Aziza, Mathieu Moreau. Non-volatile SRAM memory cells based on ReRAM technology. SN Applied Sciences, 2020, 2 (9), 10.1007/s42452-020-03267-z . hal-03504289

HAL Id: hal-03504289

<https://hal.science/hal-03504289>

Submitted on 29 Dec 2021

HAL is a multi-disciplinary open access archive for the deposit and dissemination of scientific research documents, whether they are published or not. The documents may come from teaching and research institutions in France or abroad, or from public or private research centers.

L'archive ouverte pluridisciplinaire **HAL**, est destinée au dépôt et à la diffusion de documents scientifiques de niveau recherche, publiés ou non, émanant des établissements d'enseignement et de recherche français ou étrangers, des laboratoires publics ou privés.

Non-Volatile SRAM Memory Cells based on ReRAM Technology

Hussein Bazzi^{1,2}, Adnan Harb¹, Senior Member, *IEEE*, Hassen Aziza², Mathieu Moreau²

Department of Electrical and Electronics Engineering

¹Lebanese International University

Mouseitbeh, Mazraa, Beirut, Lebanon

²IM2NP-UMR CNRS 7334, Aix-Marseille University, Marseille, France

Corresponding author: adnan.harb@liu.edu.lb

Abstract—*Static Random-Access Memories (SRAMs) are very common in today's chip industry due to their speed and power consumption but are classified as volatile memories. Non-Volatile SRAMs (nvSRAMs) combine SRAM features with non-volatility. This combination has the advantage to retain data after power off or in the case of power failure, enabling energy-efficient and reliable systems under frequent power-off conditions. In this work, several nvSRAMs architectures based on Oxide Random-Access Memory (OxRAM) technology are presented and compared. OxRAMs are non-volatile memories considered as a subset of Resistive RAM (ReRAM) technology.*

Index Terms—*1T1R ReRAM, Static Random-Access Memory (SRAM), Non-Volatile Static Random-Access Memory (nvSRAM), Power Consumption.*

I. INTRODUCTION

The rapid growth in the field of portable electronic devices has been driven by integrated circuits continuous decrease in power consumption and cost. In this context, emerging memories and specifically Non-Volatile Memories (NVM) based on new materials and technologies have flourished [1]. The promising flow of NVM technology is expected to be the pioneer technology for the upcoming years [2]. In the recent years, the interest shifted from Flash memories to alternative NVM technologies based on new materials. These technologies show signs of future success towards enhancing the memory performance and increasing the capability of scaling [3]. Among the different alternative memory technologies, Resistive RAM based on metal oxides known as Oxide Random-Access Memory (OxRAM) have attracted a lot of attention [4]. Indeed, OxRAM devices feature faster READ/WRITE operations, better energy conservation and high endurance than classical Flash memories [5].

Traditional Static Random-Access Memories (SRAMs) are volatile, which is a major handicap regarding power-down operation where non-volatile memory is needed. OxRAM can be an integral part of the well-known SRAM. This combination called non-volatile SRAM (nvSRAM) integrates both structures in a single cell [6]. nvSRAM offers a direct bit-bit connection to guarantee a fast switching speed and a high rate of data transfer [7]. This concept allows the structure to achieve genuine data retention and low power consumption with small area. Moreover, the non-volatile capability is

integrated on the BackEnd-Of-Line (BEOL) [8]. Classical low power techniques including clock gating and power gating are commonly used for MCUs power reduction. Clock gating technique is used for reducing dynamic power by controlling switching activities on the clock path [9]. In the case of power gating, certain areas of the chip are idle and other parts are activated only for certain operations [10]. In this context, emerging Non-Volatile Memory (NVM) devices can act as key enablers in the development of ultra-low power (ULP) MCUs [11]. This development opens new area of improvements in the ability of computing and energy conservation of existing systems including IoT applications [11]. The rapid expansion of emerging memories reached SRAMs technology that really needs a push to overcome serious problems including the reduction of the power supply and in the transistor size, leading to an increase of leakage currents [12].

Proposed nvSRAM designs are implemented in a high voltage 130-nm technology from STMicroelectronics. In section II, the basic OxRAM model used in this work is presented along with the 1T1R OxRAM cell considered in this study. Section III proposes a detailed overview of OxRAM-based nvSRAM structures, with a deep looking on the ability of the nvSRAM to STORE and RESTORE data. In section IV, a discussion and a comparison of the different nvSRAM cells are proposed. At the end of this paper, the conclusion summarizes all the concepts of previous sections.

II. RERAM TECHNOLOGY

A. OxRAM Model

The OxRAM model approach used in this work is based on the formation and destruction of oxygen vacancies by the induced electric field inside the insulator layer [13]. In this model, SET and RESET (operations used to switch between high and low resistive states) are constantly managed by a distinct equation where the radius of the conductive filament controls the resistance [14]. This equation is given as:

$$\frac{dr_{CF}}{dt} = (r_{CFmax} - r_{CF}) \cdot 10^{\beta_{RedOx}} \cdot e^{-\frac{Ea - q \cdot \alpha_{red} \cdot V_{cell}}{k_b \cdot T}} - r_{CF} \cdot 10^{\beta_{RedOx}} \cdot e^{-\frac{Ea + q \cdot \alpha_{ox} \cdot V_{cell}}{k_b \cdot T}} \quad (1)$$

where β_{RedOx} is the nominal oxide reduction rate, E_a is the

activation energy, α_{red} and α_{ox} are the transfer coefficients (ranging between 0 and 1), k_b is the Boltzmann constant, r_{CFmax} is the maximal size of the conductive filament radius, T is the temperature and V_{cell} the voltage across the cell.

Furthermore, some assumptions are considered in the model including a uniform electric field and radius of the conductive filaments. Also, the acceleration of the oxide reactions is triggered by the temperature. Lastly, two components are included in the OxRAM total current, which are the current linked to the conductive species (I_{CF}) and the current related to the conduction through the oxide (I_{OX}). The two equations for I_{CF} and I_{OX} are formulated as follow:

$$I_{CF} = \frac{V_{Cell}}{L_x} \cdot (\pi \cdot r_{CF}^2 \cdot (\sigma_{CF} - \sigma_{OX}) + \pi \cdot r_{CFmax}^2 \cdot \sigma_{OX}) \quad (2)$$

$$I_{OX} = A_{HRS} \cdot S_{Cell} \left(\frac{V_{Cell}}{L_x} \right)^{\beta_{HRS}} \quad (3)$$

where L_x is the oxide thickness, S_{Cell} is the total area of the device, σ_{OX} the oxidation rate and σ_{CF} the reduction rate. The two parameters A_{HRS} and β_{HRS} alongside the power law between the bias applied and the cell current are considered, thus I_{OX} trap assisted current can be taken into account. Finally, the total current passing through the cell is expressed as follow:

$$I_{Cell} = I_{CF} + I_{OX} \quad (4)$$

This model is calibrated on silicon (130 nm technology from STM) with no convergence issues when used in combination with CMOS technology. Also, it is considered as one of the few model taking into account the FORMING operation, which is a crucial factor when targeting the fabrication of the proposed devices. Moreover, the 130 nm technology provides High Voltage (HV) transistors needed for the FORMING operation. The need of a HV option (around 3V) prevents the use of more advanced technology nodes.

B. 1T1R Structure

The OxRAM cell consists of three layers, including the insulator layer (switching layer) working as the storage medium which is located between two metallic electrodes (top electrode TE and bottom electrode BE). This Metal-Insulator-Metal (MIM) structure is integrated over a Metal 4 copper layer (Cu) as shown in Fig. 1(a). First, the TiN BE is deposited. Then, a 10nm-HfO₂/10nm-Ti/TiN stack is added to form a capacitor-like structure [15].

One of the common selector used with ReRAM devices is the CMOS transistor. In this context, the 1 transistor-1 resistor (1T1R) structure has been widely used, where the OxRAM cell is connected on the top of the transistor as shown in Fig. 1(b). In addition, the transistor controls the compliance current passing through the OxRAM cell during programming operations to prevent memory cell damage.

Fig. 2 (a) and (b) present 1T1R OxRAM I-V characteristics in linear scale and logarithmic respectively

extracted from actual OxRAM devices [16]. The principle operation of OxRAM based memory cells consists of several stages [17]. The first step is the Forming operation which is executed once in the life of OxRAM cell, where a high voltage is induced to switch from High Resistance State (HRS or pristine state) to Low Resistance State (LRS) [18]. After Forming, the cell can be switched between HRS and LRS by applying specific voltages across the electrodes of the OxRAM cell (i.e. V_{SET} and V_{RESET}) [19]. Regarding reliability, as demonstrated in [20], SET/RESET endurance was evaluated up to 10^8 cycles showing that the oxide-based technology is in agreement with SRAM operation. Fig. 3 presents the evolution of the ON/OFF resistance ration during cycling.

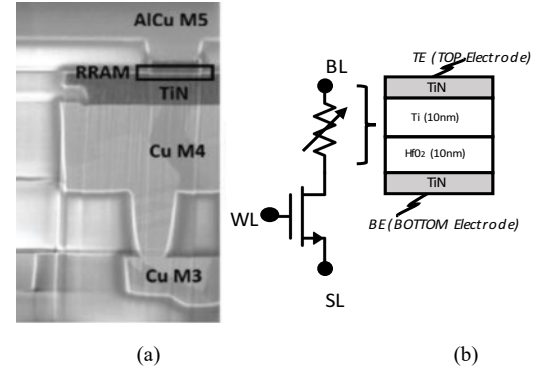


Fig. 1. (a) MIM structure and (b) Basic 1T-1R OxRAM cell

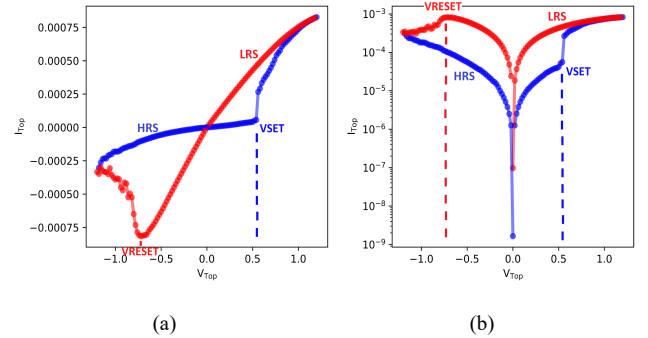


Fig. 2. I-V characteristic of the OxRAM model in (a) linear and (b) log scale

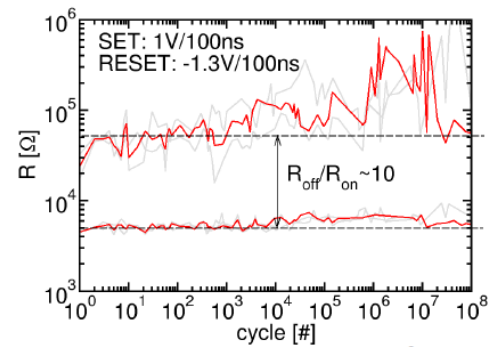


Fig. 3. SET/RESET endurance evaluated up to 10^8 cycles [20].

Based on the linear curve presented in Fig. 2 (a), V_{SET} value needed to switch to LRS state is equal to 0.57 V, while the V_{RESET} value required to switch back to HRS state is equal to -0.7 V. Note that the log curve is the classical representation of the OxRAM I-V hysteresis as it amplifies low current values.

C. 1T1R OxRAM Cell Simulation

The OxRAM model used for simulations is a compact model calibrated on silicon well suited to simultaneously describe SET and RESET operations [21]. Fig. 4 presents timing waveform of the 1T1R cell presented in Fig. 1(b) during FORMING, RESET & SET operations. The duration of these 3 operations are 13 μ s, 4 μ s and 1 μ s respectively.

$V_{(TE, BE)}$ represents the voltage across the OxRAM device. The voltage at the gate of the transistor $V_{(WL)}$ is kept high. During FORMING, the voltage at the top electrode $V_{(BL)}$ is also set high (3.5 V), and the voltage at the bottom electrode $V_{(SL)}$ is 0V. After FORMING, OxRAM device is RESET with $V_{(BL)} = 0V$ and $V_{(SL)} = 2.7V$. During the SET operation, $V_{(BL)}$ is set to 1.8V.

III. NON-VOLATILE SRAM

A. NVSRAM memory cells

As already mentioned in the introduction, one of the solution to reduce/eliminate standby power in SRAM cells since it to turn the traditional volatile SRAM non-volatile. The addition of this feature is important to eliminate the standby leakage currents. Indeed, the memory can operate in a conventional way in active mode and can be powered OFF in standby mode to prevent standby power consumption without losing its data.

In the next sections, five different types of nvSRAMs are presented. These architectures include Majumdar's 4T2R cell [22], Wei's 7T1R cell [23], Turkyilmaz's 8T2R cell [24], Sheu's 7T2R cell [25], and Chiu's 8T2R cell [26].

Each nvSRAM cell is based on the conventional SRAM structure. The conventional SRAM structure follows the cross coupled inverters structure presented in Fig. 5. The 3 main operations in a SRAM are HOLD, READ and WRITE. At an SRAM memory array level, rows are called Word Lines (WLs) and columns are called Bit Lines (BLs). WLs are connected to the gates of the select transistors (M5 and M6).

WRITE and READ operations in the memory cells are accomplished through the bit lines. During a HOLD operation, the WL is deactivated to disconnect BL and BLb from the SRAM cell. As a result, data is held in the latch structure on nodes Q and Qb. When WL is activated, READ and WRITE operations can be executed.

B. 4T2R Cell [22]

The 4T2R nvSRAM cell [22] is presented in Fig. 6. It consists of 2 OxRAMs, 4 Transistors, where M3 and M4 act as access transistors connecting the bit lines to Q and Qb nodes. FORMING operation is mandatory before operating the nvSRAM. Note that OxRAM devices R1 and R2 need a high voltage on the top electrodes to be formed.

Note that a STORE operation (SET or RESET operation of the OxRAM cell) is associated with a WRITE operation. During WRITE/STORE, the bit lines are connected to the nodes Q and Qb. The potential difference between TE (Q or Qb) and BE (PL line) of the OxRAM element will either induce a SET (ON state) or RESET (OFF state) operation of the cell. After WRITE/STORE operation the cell data remains unchanged as well as the cell resistances provided that no sufficient voltage potential difference is seen across the OxRAM cells. After power shutdown, the nvSRAM last state can be restored as the data is saved in a non-volatile resistance value. The restored nvSRAM value can be checked during a READ operation after powering on the cell. PL line is connected to V_{DD} and a certain amount of current will pass through the OxRAM devices depending on their resistance values.

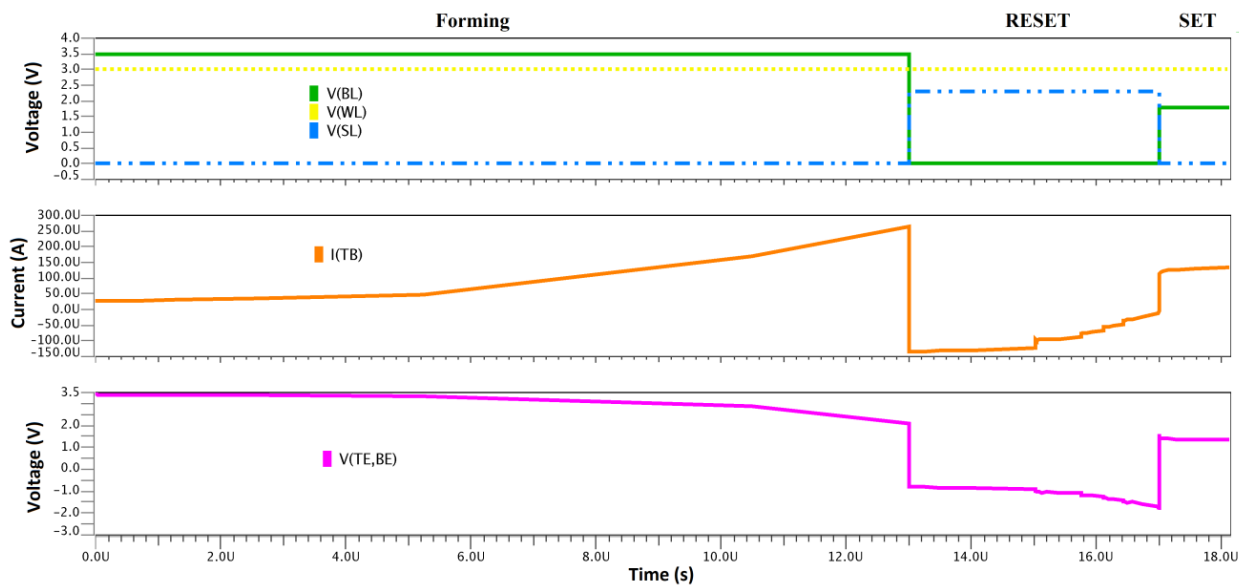


Fig. 4. 1T1R timing waveforms

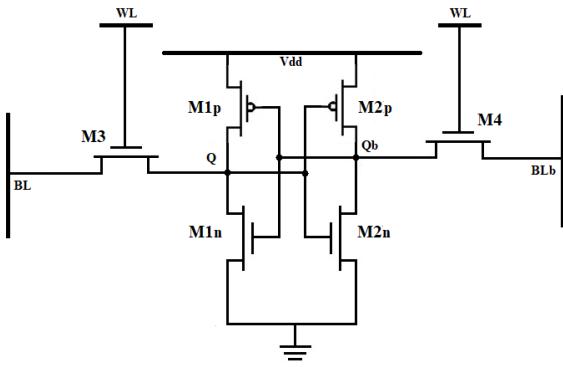


Fig. 5. 6T SRAM Cell

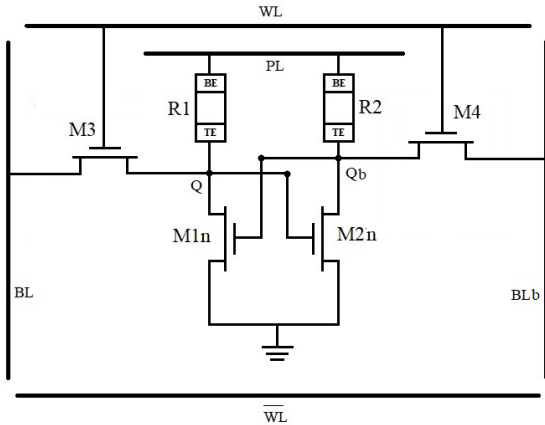


Fig. 6. 4T2R nvSRAM Cell

Fig. 11 presents timing waveforms of the 4T2R Cell. During FORMING, BL and BLb are high and WL and PL low. After FORMING, R1 is RESET while R2 stays in LRS state with BLb and PL high and BL low. The next following 2 steps are Pre-charge and READ to check the memory state. BL and BLb are pre-charged to $V_{DD}/2$ and PL is set to 1V to not affect R1 and R2 resistance values during the next read operation.

During READ, WL is turned ON thus the data on the nodes can be transmitted to the bit lines to reach the reading circuitry. After that, R1 device is SET and R2 is RESET consecutively following the same programming scheme of the previous STORE operation. Since the nvSRAM is non-volatile, the memory cell is powered down to test the ability of the cell to recover the data. The shutdown is followed by a RESTORE operation where a 1V voltage is applied to PL to get the data back to the storage nodes. After RESTORE, a Pre-charge and READ are performed to check Q and Qb values.

C. 7T1R cell [23]

The 7T1R nvSRAM cell [23] is presented in Fig. 7. The structure of this cell consists of 1 OxRAM, 7 Transistors, including 2 CMOS inverters and 2 access transistors. M5 access transistor acts as switch controlling the STORE operation. In this configuration, one OxRAM device is directly connected to the memory nodes Q which is used to store logic states “0” and “1”. The resistance of the OxRAM

switches between HRS and LRS depending on the data stored at nodes Q and Qb. As the previous structure, FORMING is executed at the beginning but only through BL since there is only 1 OxRAM device.

During the STORE operation, the data on the bit line is transferred to the node Q, while CTRL1 is high and CTRL2 is grounded. For instance, if the node Q data is “1”, the potential difference across the OxRAM changes the resistance from HRS to LRS. This setup is mandatory to program the device depending on node Q voltage. At the end of this operation, the resistance state of the OxRAM matches the logic states stored at the data nodes (Q and Qb). Note that before STORE, node Q is grounded to discharge any voltage left at this node.

During power-down stage, all the voltage sources are shutdown. During RESTORE operation, the current from CTRL2 passes through the OxRAM device depending on the resistive state. For instance, if the OxRAM is in LRS, the node Q stays at “1” and Qb is discharged through the NMOS transistor M2n.

During READ operation, WL and CTRL1 are high, thus the current passes in the OxRAM device depending on its resistance value. Node Q is connected to BL to sense the memory cell state.

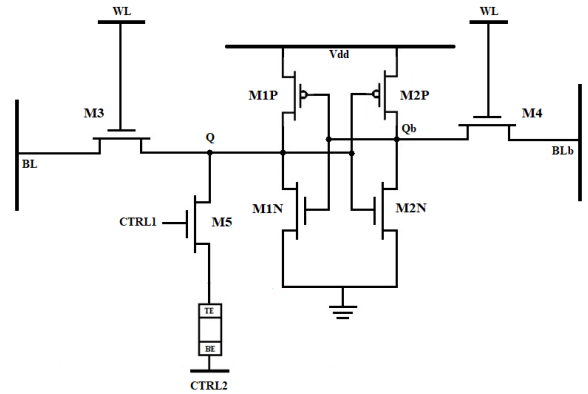


Fig. 7. 7T1R nvSRAM Cell

Timing waveforms of the 7T1R cell presented in Fig. 12 differ from the 4T2R cell as WRITE and STORE operations are executed separately. During FORMING, BL is high with WL and CTRL1 set high. RESET is preceded by a WRITE “0” operation where node Q data is stored in the OxRAM device. Note that this the 7T1R architecture can work as a traditional SRAM when M5 is OFF (i.e. independently from the OxRAM cell). BL is high during FORMING and WRITE “1” operation. CTRL1 is high during Forming, SET, RESET and RESTORE operations. The value of the current passing through R1 $I(TB)$ is only considered when CTRL1 (V_{ctrl}) is ON, since no current flows in the device when it is OFF. $I(TB)$ increases gradually during FORMING.

RESET operation is performed by applying a high voltage on CTRL1 and CTRL2, while WL is grounded. During this operation, $I(TB)$ decreases to nearly 0V since the OxRAM switched to the HRS. On the other hand, during SET $I(TB)$ increases as the OxRAM is in LRS state. In RESTORE,

CTRL1 is high and the restore voltage is applied on CTRL2 where the current $I(TB)$ will pass through the OxRAM depending on the resistive state (HRS or LRS). After RESTORE, a Pre-charge and READ are performed to check Q and Qb values.

D. 8T2R Cell [24]

The design proposed in Turkyilmaz paper [24] is very similar to 7T1R cell [23], as two OxRAM devices are used instead of one. However, OxRAMs are accessed using two transistors M3 and M4 controlled by CTRL1 signal as shown in Fig. 8. Regarding the operation principle, the same procedure used for the 7T1R structure can be followed but considering 2 OxRAM cells. SET and RESET are performed by activating M5 and M6. In case of SET, CTRL1 is high and CTRL2 is grounded and according to the data stored in the nvSRAM cell, either R1 or R2 is set to LRS. During RESET CTRL2 is SET to V_{DD} and according to the data stored in the nvSRAM cell, either R1 or R2 is set to HRS.

During RESTORE, if R1 is in LRS, node Q is “refreshed” with logic ‘1’. If R1 is in HRS, node Q is “refreshed” with logic ‘0’. R2 follows the same procedure.

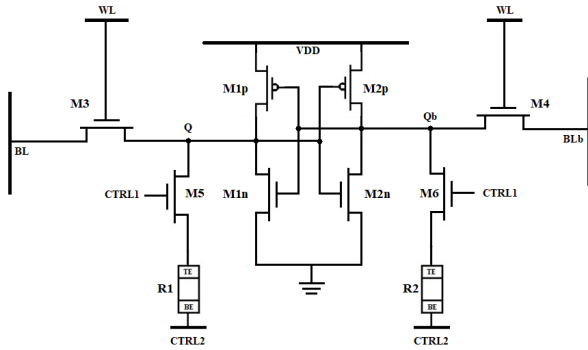


Fig. 8. 8T2R nvSRAM Cell

After RESTORE, R1 and R2 are disconnected from the rest of the circuit and the SRAM is not effected by the OxRAM cells (i.e. M5 and M6 isolate the OxRAM from the SRAM core to avoid the degradation of the cell performance in the normal mode operation).

Timing waveforms presented in Fig. 13 are practically the same as the 7T1R memory cell [23], but since the 7T1R design is built using 2 OxRAM devices, 2 FORMING operations are needed. During the FORMING stage, BL is set high to form OxRAM R1 (current $I1(TB)$ increases). Then, BLb is set high to form OxRAM R2 (current $I2(TB)$ increases). After FORMING, the 8T2R cell follows the same programming routine as the 7T1R cell but considering two OxRAM devices instead of one. Currents $I1(TB)$ and $I2(TB)$ change depending on the executed operation. During RESTORE, CTRL1 is ON and CTRL2 is set to 1V. During READ operation, WL and CTRL1 are set high.

E. 7T2R Cell [25]

The design proposed in Sheu paper [25] is close to 8T2R cell, excepted that a single signal SWL controls STORE/RESTORE operations as presented in Fig. 9. The

8T2R consists of 2 OxRAMs, 7 transistors including 2 CMOS inverters and 3 access transistors. M_{NSW} transistor controls STORE/RESTORE operations. Also, OxRAMs bottom electrodes (BE) are connected to M3 and M4 which connect the cell to the bit lines.

FORMING operation in the 7T2R cell follows this sequence: WRITE “0” on node Q, R_L FORMING, WRITE “1” on node Q, and R_R FORMING. Note that FORMING operation is performed through BL for both OxRAMs.

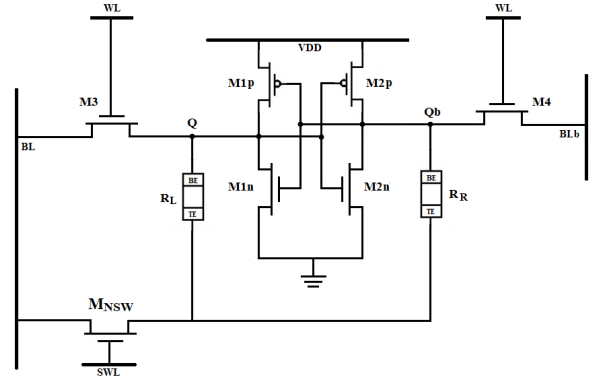


Fig. 9. 7T2R nvSRAM Cell

During STORE, OxRAMs resistance changes from LRS and HRS respectively depending on Q and Qb node voltages provided that SWL signal is set high. During READ operation, WL is high and SWL low, disconnecting R_L and R_R from the core SRAM cell.

Timing waveforms are presented in Fig. 14. FORMING operation in 7T2R cell [25] is divided into 2 stages (R_L and R_R FORMING). The first stage starts with WRITE “0” with BL and SWL set low and WL set high. Then, R_L is formed with BL and SWL set high and WL set low. In the second stage, R_R FORMING is achieved starting with WRITE “1” operation with BL and WL set high and SWL set low. Note that BL, SL and SWL have the same programming levels during R_L and R_R FORMING.

RESET is performed after WRITE “1” operation, where $I1(TB)$ decreases to approximately 0V ($R1$ in HRS state). WL is high and SWL is low during WRITE, and the opposite during RESET operation. WRITE “0” operation is needed before SET. WL and SWL follows the same pattern as in (WRITE/RESET) sequence. During programming, WRITE “0” on the node Q and “1” on Qb are executed simultaneously. During the STORE operation, BL is high to SET $R1$ and low to RESET $R2$. Note that BL is the only bit line participating in this operation. During RESTORE, the data retained at node Q is “1” if the OxRAM device is in LRS state and “0” if it is in HRS state. During READ operation, WL is set high and SWL is set low.

F. 8T2R Cell [26]

The design proposed by Chiu [26] is based on the 7T2R structure presented in Fig. 9 except that the top electrodes of the OxRAM cells are connected to the different bit lines. The 8T2R cell is depicted in Fig. 10.

The proposed nvSRAM cell spares on control signal as M5 and M6 transistors are controlled by BL and BLb respectively. In this design, FORMING is executed through both bit lines (BL and BLb).

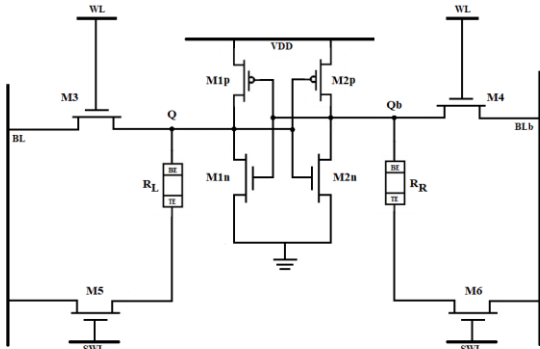


Fig. 10. 8T2R nvSRAM Cell (CHIU)

After FORMING, the corresponding bit line is used to STORE (SET/RESET) data on the OxRAM. The switch-line (SWL) is grounded to turn off the selector transistors connected to the bit lines and to prohibit any potential disturbance that affects the stability of the SRAM cell. FORMING operation in this design is performed through the bit lines BL and BLb connected to R_L and R_R respectively. During RESTORE, data stored on the OxRAM devices are recalled to the nodes (Q and Qb).

Timing waveforms of this structure are close to that of 7T2R cell [26] as shown in Fig. 15. During FORMING both BL and BLb are high to form the 2 OxRAM devices at the same time, thus the currents (I₁(TB) and I₂(TB)) increase simultaneously. The currents I₁(TB) and I₂(TB) will react depending on the operation executed.

BLb is low during WRITE "1", and high during WRITE "0". During RESTORE, SWL is high and WL is low with restore voltage is applied at the bit lines.

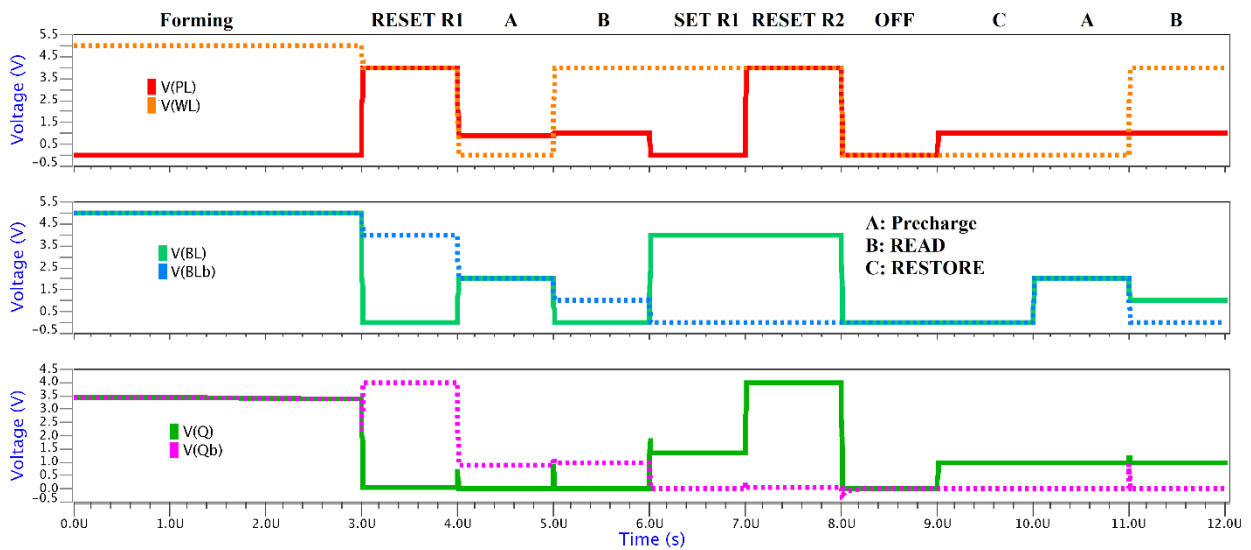


Fig. 11. 4T2R Timing Waveforms

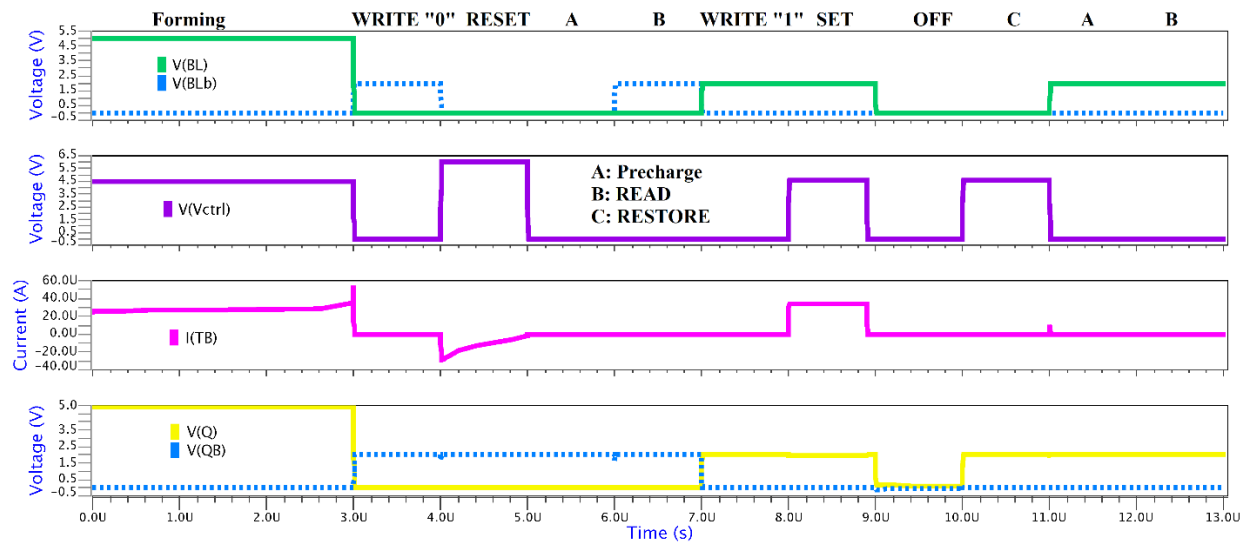


Fig. 12. 7T1R Timing Waveforms

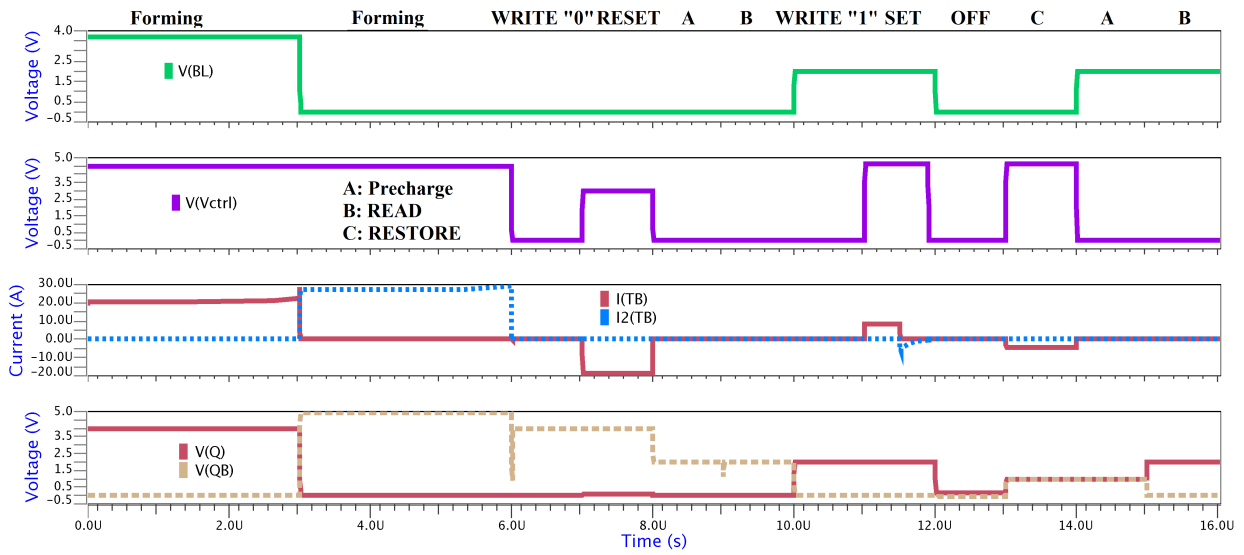


Fig. 13. 8T2R Timing Waveforms

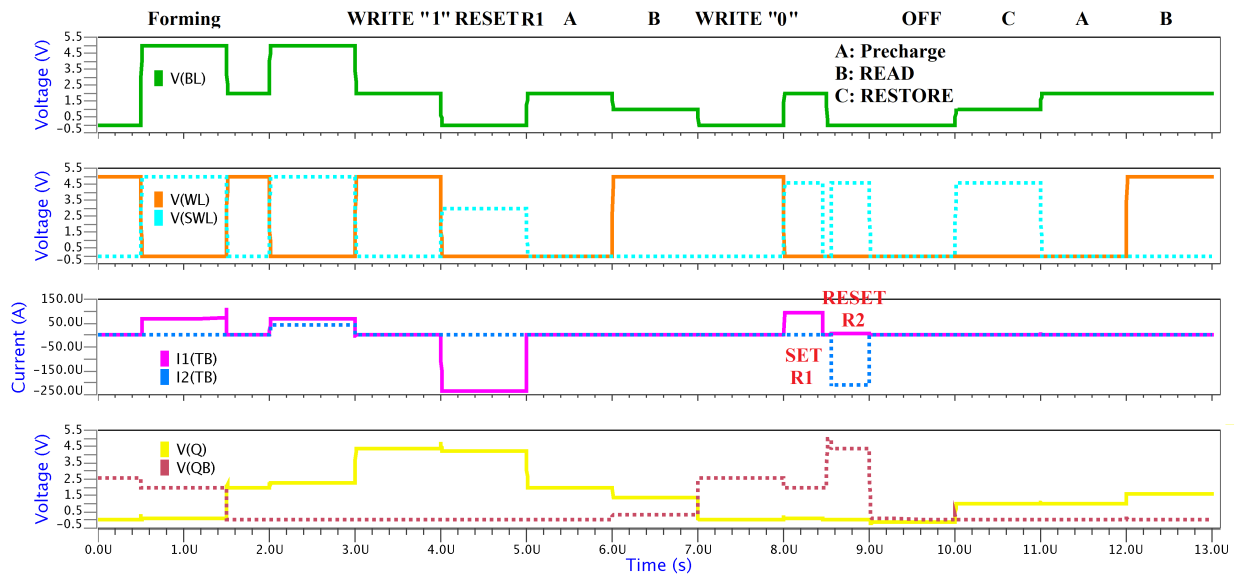


Fig. 14. 7T2R Timing Waveforms

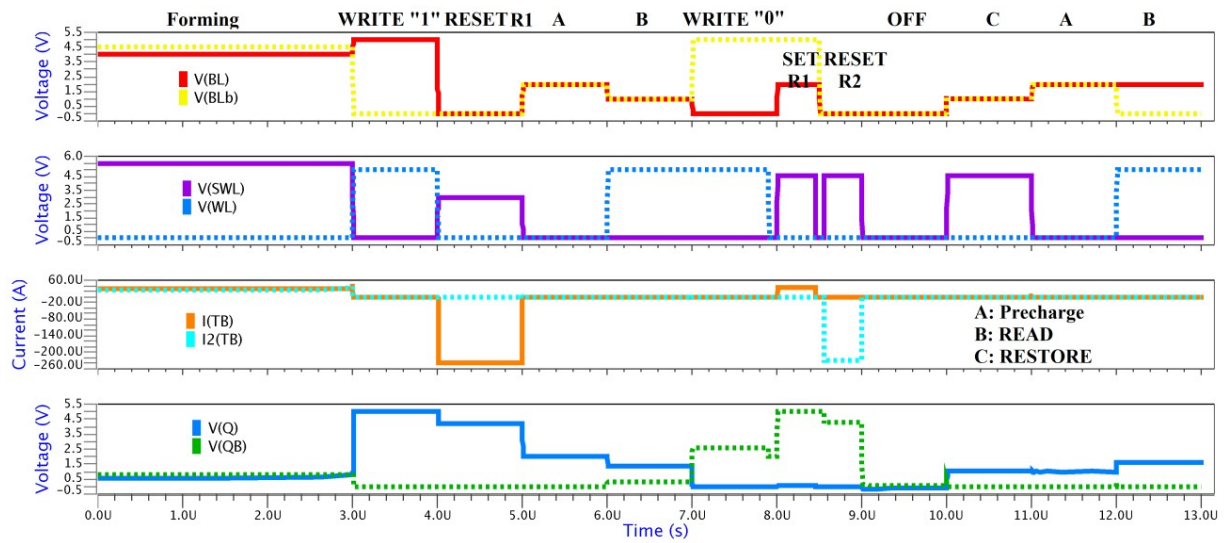


Fig. 15. 8T2R Timing Waveforms (CHIU)

IV. STRUCTURE COMPARAION & DISCUSSIONS

In this section, 5 nvSRAM cells are discussed and compared showing their advantages and limitations. Table I illustrates advantages/drawbacks of all nvSRAMs in terms of STORE/RESTORE time, RESTORE method, non-volatility mode, STORE/RESTORE energy, area and silicon verification.

TABLE I
COMPARISON BETWEEN NVSRAM DESIGNS IN TERM OF
DIFFERENT PARAMETERS

	4T2R [22]	7T1R [23]	8T2R [24]	7T2R [25]	8T2R [26]
STORE Time	1.45ns	0.24ns	0.24ns	1ns	0.8ns
RESTORE Time	20ps	0.22ns	0.22ns	0.37ns	0.36ns
RESTORE Method	Differ- -ential	Single- -ended	Differ- -ential	Differenti- -al	Differenti- -al
Non-Volatility	Real- -time	Before -Shutdown	Before -Shutdown	Before -Shutdown	Before -Shutdown
STORE Energy	4.9nJ	0.3nJ	0.5nJ	0.9nJ	0.8nJ
RESTORE Energy	30fJ	50fJ	80fJ	0.25fJ	0.52fJ
Forming Energy	1.7nJ	0.35nJ	0.77nJ	1nJ	6.345nJ
Area	Small	Medium	Large	Medium	Large
Silicon Verified	No	No	No	Yes	Yes

4T2R nvSRAM cell [22] presents a real-time non-volatility with both WRITE and STORE executed simultaneously. This cell follows the differential sensing approach as RESTORE method (2 OxRAMs). The structure of this design has a low area overhead, since the OxRAM devices replace the pMOS transistors. STORE/RESTORE times measured for this cell are 1.45ns and 20ps respectively. This cell is slower than conventional 6T SRAM due to programming of the OxRAM cell which occurs during each WRITE cycle. On the other hand, this design offers a real time non-volatility, and not a last-bit (or power-down) non-volatility as a trade-off for speed drawback. Also, this structure suffers from high power consumption as a STORE operation comes with a WRITE operation. STORE energy including SET and RESET operations is 4.9nJ. RESTORE energy is around 30fJ. The energy dissipated by the OxRAM device during Forming is 1.7nJ.

7T1R [23] and 8T2R [24] nvSRAM cells are based on 6T SRAM core unlike 4T2R cell [18]. Although 7T1R cell [23] suffers from a slight increase of the variability in resistance and process, but this issue does not corrupt the normal operation of the nvSRAM design. The advantage of 7T1R cell [23] is its low power consumption and area, knowing that only one OxRAM is used. The STORE energy is 0.3nJ [23] which is slightly less than [24] with 0.5nJ. Forming energy for the 7T1R cell is approximately half of that for 8T2R. Both structures scored similar numbers for RESTORE energy (50 and 80fJ). Regarding STORE/RESTORE times, they follow

the same scheme with 0.24ns and 0.22ns respectively. The asymmetric design (single-ended sensing as RESTORE method) makes the structure more susceptible READ disturb, but it is not considered a significant drawback. 8T2R cell [24] is more consistent in the READ operation, but at the expense of more area and power consumption (2 OxRAM devices).

7T2R [25] and 8T2R [26] non-volatile SRAMs have achieved fast bit-to-bit parallel STORE/RESTORE operations (1ns and 0.37ns respectively), low energy requirements, and low READ/WRITE V_{DD} enabling mobile chips to achieve low active-mode power consumption. Furthermore, low-energy STORE/RESTORE operation (0.9nJ & 0.25fJ for [25], and 0.8nJ & 0.52fJ for [26]) prevents data loss in mobile devices resulting from rapid power failure. Forming energy for [25] is 1nJ and 6.345nJ for [26].

Finally, it should be noted that the STORE time of the OxRAM devices is not constant as it depends on the programming conditions which are different for each memory cell. The same applies for the Forming time.

V. CONCLUSION

SRAM memory cells based on OxRAM are proposed as an enhanced structure to boost SRAM performances in terms of power consumption. In this context, the 1T1R OxRAM structure is used as a basic cell in different nvSRAM topologies, offering a large band of benefits while keeping a low design complexity. nvSRAM architectures have been explored, showing their advantages and drawbacks. As a conclusion, it appears that 4T2R nvSRAM cell offers real time non-volatility with low area with more power consumption compared to other nvSRAM architectures. The other architectures present a last-bit non-volatility with low power consumption.

ACKNOWLEDGMENT

I would like to acknowledge the support of the Lebanese International University, Aix-Marseille University, and the support of Campus France (Eiffel scholarship).

FUNDING

This study was funded by the Lebanese International University, Aix-Marseille University, and Campus France.

CONFLICT OF INTEREST

The authors declare that they have no conflict of interest.

REFERENCES

- [1] Meena, J.S., Sze, S.M., Chand, U. et al. Nanoscale Res Lett (2014) 9: 526.
- [2] S. Hamdioui et al., "Memristor based memories: Technology, design and test", Design & Technology of Integrated Systems in Nanoscale Era (DTIS), 9th IEEE International Conference On, 2014.
- [3] Ielmini Daniele, "Resistive Switching Memories Based on Metal Oxides: Mechanisms, Reliability and Scaling." Semiconductor Science and Technology, vol. 31, no. 6, 2016.
- [4] D. Garbin et al., "HfO₂-Based OxRAM Devices as Synapses for Convolutional Neural Networks," in IEEE Transactions on Electron Devices, vol. 62, no. 8, pp. 2494-2501, Aug. 2015.

- [5] M. Bocquet et al., "Robust Compact Model for Bipolar Oxide-Based Resistive Switching Memories," in IEEE Transactions on Electron Devices, vol. 61, no. 3, pp. 674-681, March 2014.
- [6] H. Bazzi et al., "Design of Hybrid CMOS Non-Volatile SRAM Cells in 130nm RRAM Technology," 2018 30th International Conference on Microelectronics (ICM), Sousse, Tunisia, 2018, pp. 228-231.
- [7] Xie, Y. (2014). Emerging Memory Technologies: Design, Architecture, and Applications. New York, NY: Springer.
- [8] M. Chang et al., "Challenges at circuit designs for resistive-type Nonvolatile memory and nonvolatile logics in mobile and cloud applications," 2014 12th IEEE International Conference on Solid-State and Integrated Circuit Technology (ICSICT), Guilin, 2014, pp. 1-4.
- [9] L. Sterpone et al., "A new reconfigurable clock-gating technique for low power SRAM-based FPGAs," 2011 Design, Automation & Test in Europe, Grenoble, 2011, pp. 1-6.
- [10] P. Singh et al., "Ultra-Low Power, Process-Tolerant 10T (PT10T) SRAM with Improved Read/Write Ability for Internet of Things (IoT) Applications," J. Low Power Electron. Appl. 2017, 7, 24
- [11] C. Dou et al., 2017 IEEE 12th International Conference on ASIC (ASICON).
- [12] J.-M. Portal, et al., "An Overview of Non-Volatile Flip-Flops Based on Emerging Memory Technologies," Journal of Electronic Science and Technology, vol. 12, no. 2, 2014, pp. 173-181.
- [13] M. Bocquet et al., "Robust Compact Model for Bipolar Oxide-Based Resistive Switching Memories," in IEEE Transactions on Electron Devices, vol. 61, no. 3, pp. 674-681, March 2014.
- [14] A. J. Bard and L. R. Faulkner, Electrochemical methods: fundamentals and applications, J. Wiley and S. Inc., Eds., New York, 2001.
- [15] G. Molas, et al., "Resistive Memories (RRAM) Variability: Challenges and Solutions," ECS Transactions, vol. 86, no. 3, pp. 35-47, 2018.
- [16] M. Bocquet, D. Deleruyelle, H. Aziza, C. Muller and J. Portal, "Compact modeling solutions for OxRAM memories," 2013 IEEE Faible Tension Faible Consommation, Paris, 2013, pp. 1-4.
- [17] H Aziza et al., "Resistive RAMs as analog trimming elements," Solid-State Electronics 142, 52-55.
- [18] P Canet et al., "Impact of resistive paths on NVM array reliability: Application to Flash & ReRAM memories," Microelectronics Reliability 64, 36-41.
- [19] F. Nardi et al., "Resistive Switching by Voltage-Driven Ion Migration in Bipolar RRAM Part I : Experimental Study," IEEE Transactions on Electron Devices, vol. 59, no. 9, pp. 2461– 2467, 2012.
- [20] B. DeSalvo et al., "Emerging resistive memories for low power embedded applications and neuromorphic systems," 2015 IEEE International Symposium on Circuits and Systems (ISCAS), Lisbon, 2015, pp. 3088-3091.
- [21] B. Hajri et al., "Oxide-based RRAM models for circuit designers: A comparative analysis," 2017 12th International Conference on Design & Technology of Integrated Systems In Nanoscale Era (DTIS), Palma de Mallorca, 2017, pp. 1-6.
- [22] S. Majumdar et al., "Hybrid CMOS-OxRAM based 4T-2R NVSRAM with efficient programming scheme," 2016 16th Non-Volatile Memory Technology Symposium (NVMTS), Pittsburgh, PA, 2016, pp. 1-4.
- [23] W. Wei et al., "Design of a Nonvolatile 7T1R SRAM Cell for Instant-on Operation," in IEEE Transactions on Nanotechnology, vol. 13, no. 5, pp. 905-916, Sept. 2014.
- [24] O. Turkyilmaz et al., "RRAM-based FPGA for "normally off, instantly on" applications," 2012 IEEE/ACM International Symposium on Nanoscale Architectures, Amsterdam, 2012, pp. 101-108.
- [25] S. Sheu *et al.*, "A ReRAM integrated 7T2R non-volatile SRAM for normally-off computing application," 2013 IEEE Asian Solid-State Circuits Conference (A-SSCC), Singapore, 2013, pp. 245-248.
- [26] P. Chiu et al., "Low Store Energy, Low VDDmin, 8T2R Nonvolatile Latch and SRAM With Vertical-Stacked Resistive Memory (Memristor) Devices for Low Power Mobile Applications," in IEEE Journal of Solid-State Circuits, vol. 47, no. 6, pp. 1483-1496, 2012.